ACS OMEGA

http://pubs.acs.org/journal/acsodf

Article

Comparison between Chlorine-Shared and π−Halogen Bonds Involving Substituted Phosphabenzene and ClF Molecules

Dipankar Sutradhar, Sumitra Bhattarai, Salma Parveen, and Asit K. Chandra*

Cite This: *ACS Omega* 2020, 5, 24095−24105

Read Online

ACCESS | Metrics & More | Article Recommendations | Supporting Information

ABSTRACT: Ab initio MP2/aug-cc-pVTZ calculations have been carried out in order to study the nature of P···Cl halogen bonding interaction between a phosphorus atom in an aromatic ring in para-substituted phosphabenzene (PPBZ) and ClF molecule. The interaction of PPBZ with ClF results in two different types of complexes: (i) complex formation through the chlorine-shared halogen bond (T1-X-PPBZ·ClF) and (ii) complex formation *via* halogen−π interaction (T2-X-PPBZ·ClF). T1-X-PPBZ·ClF complexes are found to be more stable than the T2-X-PPBZ·ClF complexes. This work also presents a general criterion to distinguish a chlorine-shared halogen bond from a traditional halogen bond and sheds light on the formation of the chlorine-shared halogen bond. The binding energy of T1-X-PPBZ·ClF complexes correlates well with the negative electrostatic potential of the P atom and PA value of the substituted PPBZ. The properties of both T1-X-PPBZ·ClF and T2-X-PPBZ·ClF complexes are analyzed using atom-in-molecule, natural bond orbital, and symmetry-adapted perturbation theory calculations. The variation of the Cl−F bond distances and the redshifts of the ν(ClF) vibration resulting from the interaction with PPBZs are discussed.

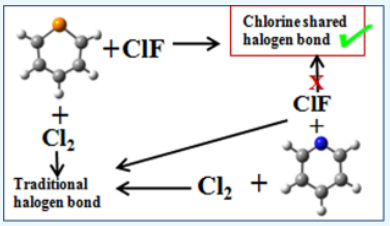

INTRODUCTION

Intermolecular association of molecules involving halogen bonds is still an area of great interest among researchers despite having been studied extensively over the last two decades. The halogen bond has a diverse range of applications in areas such as crystal engineering, polymerization, catalysis, liquid crystals, biomedical fields, and so forth.[1−7] The vital role of the halogen bond is also evident in many chemical and enzymatic reactions, molecular recognition, and synthesis of new functional materials and several useful drugs. The origin of the halogen bond is based on the σ-hole formalism as proposed by Clark et al.[8] Recently, various noncovalent interactions like chalcogen bond, pnicogen bond, and tetrel bond are also found to be associated with σ-hole.[9−12] There is a lot of available work reporting the frequently occurring traditional halogen bond in diverse areas of chemistry. Interestingly, apart from the traditional halogen bond, there exists another type of bond called the "chlorine-shared" and "ion-pair" halogen bond, which has received much attention because of its unique nature of interaction.[13−20] A few studies were carried out on the cooperative effect of the chlorine-shared halogen bond as well.[21,22] Del Bene et al. studied the "chlorine-shared" halogen bonds on numerous occasions, first, by involving CNX and ClF molecules and later with various phosphine derivatives and mixed halogens.[13,14,18−20] Initially, they used Steiner−Limbach relationship between $r_1 - r_2$ and $r_1 + r_2$ (r_1 is F−Cl distance and r_2 is Cl−C distance) in complexes of FCl···CNX (X = CN, NC, NO_2, F, CF_3, Cl, Br, H, CCF, CCH, CH_3, SiH_3, Li, and Na) to classify these halogen bonds. Traditional halogen bonds are characterized with a negative value of $r_1 - r_2$ and small interaction energy, while chlorine-shared and ion-pair halogen bonds generally have a positive $r_1 - r_2$ value Moreover, ion-pair halogen bonds show much bigger interaction energy than chlorine-shared ones. They have further clarified that chlorine-shared halogen bonds are not always associated with the positive $r_1 - r_2$ value, but a greater elongation of the ClF bond and higher binding energy can be taken as better parameters for distinguishing chlorine-shared halogen bonds. For example, in one of their works,[17] the P···Cl bond of FCl·PCLi and FCl·PCNa complexes were classified as the chlorine-shared halogen bond, even though they have binding energies of 23 and 28 kJ mol^{-1} and a elongation of only 0.041 and 0.069 Å of the ClF bond.

The halogen bond involving electron donors such as O, N, and S bases has been studied quite extensively both experimentally and theoretically.[23−27] However, halogen bonds involving P as the electron donor has not been explored to a great extent owing to its high probability of forming the P−X covalent bond because of the strong polarizing nature of the phosphorus atom.[28] Moreover, aromatic rings like pyridine, diazines, triazenes, and so forth has been used quite often for halogen-bonding studies, but aromatic rings like phosphabenzene (PPBZ) have not been explored so far. Therefore, a sincere effort has been made in this study to explore and

Received: July 26, 2020
Accepted: August 27, 2020
Published: September 14, 2020

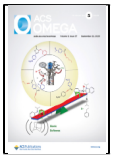

Table 1. Binding Energies and Free Energy Change of the Complexes between para Substituted PPBZ and ClF Molecules[a]

systems	ΔE		ΔG				
X=	T1-X-PPBZ·ClF	T2-X-PPBZ·ClF	T1-X-PPBZ·ClF	T2-X-PPBZ·ClF	PA	IP (eV)	$V_{s,min}$
NH_2	−42.12		−21.62		857.2	8.26	−102.22
CH_3	−41.09	−20.54	−20.06	3.75	827.2		−90.04
H	−39.43	−18.51	−18.74	6.18	814.5	10.03	−82.26
F	−33.46	−17.81	−12.46	6.61	795.0	9.34	−69.33
CN	−27.41	−15.13	−7.03	8.54	764.1	10.54	−35.15
NO_2	−26.79	−14.75	−6.24	8.54	761.8	10.58	−28.16

[a]PA, IP (eV), and $V_{s,min}$ values of PPBZ. Data are in kJ mol^{-1} and calculated at the MP2 = full/aug-cc-pVTZ level.

understand the halogen-bonding interaction, taking PPBZ as the electron donor. In fact, this is the very first theoretical study of the halogen-bonded complexes involving a phosphorus atom as a part of an aromatic ring (PPBZ) as the electron donor. Bryce and co-workers recently reported a co-crystal of triphenylphosphine with 1,3,5-trifluoro-2,4,6-triiodobenzene featuring phosphine as the halogen bond acceptor.[29] Prior to them, Teixidor et al. reported a halogen-bonded co-crystal featuring phosphine as a halogen bond acceptor in 1-diphenylphosphino-2-methyl-1,2-dicarbadodecaborane(10)-hemikis(iodine), where I_2 acts as the halogen-bond donor.[30] The importance of P···Cl contacts in crystal structure packing is further clear from the fact that a search of such contact in the Cambridge Crystal Structural Database (CSD) results with 222 hits, among which some are direct halogen bond like P···Cl contacts and few with sideways P···Cl contacts (not halogen bond). Some examples (from the CSD search) of the crystals with P···Cl contacts having CSD code are YILMAK,[31] ABERAA,[32] ADAHOE,[33] BAQJOU,[34] BAQJUA,[34] BAQKAH,[34] BAQKOV,[34] BAWDIO,[35] and so forth. Jiao et al. recently studied the traditional, chlorine-shared, and ion pair halogen-bonded complexes between various phosphine derivates and mixed halogens like Br_2, BrCl, and BrF.[15] Alkorta et al. studied the halogen-bonded complexes between XCP and ClF and classified them based on two different configurations: one forming through the FCl···P halogen bond and the other when ClF interacts with the C≡P triple bond through a perturbed π system.[17] They further showed that the nature of the halogen bond changes from traditional to chlorine-shared and the interaction energies increase, as the electron-donating ability of X increases in XCP···ClF complexes.

Reiling studied the interaction between pyridine and I_2 molecule and named them as the charge transfer (CT) complex.[36] Wang et al. studied the halogen-bonded complexes between pyridine and XY dihalogen molecules and predicted two different types of complexes; (i) one forming through π−halogen interaction and the other through σ-hole on halogen atom interacting with the lone pair of nitrogen in pyridine.[37] In a nutshell, plenty of data is already available for the complex formation between pyridine and dihalogens or interhalogens,[37−40] but there is no literature on the complex formation between PPBZ and dihalogen or interhalogens. Therefore, the results obtained for the present PPBZ·ClF complexes can be very useful in understanding the nature of halogen bonding interaction involving a P-atom in an aromatic ring. Therefore, our present study deals with the theoretical investigation on the halogen-bonded interaction between various para substituted PPBZ and ClF molecule. Both electron donor (NH_2 and CH_3) and acceptor (F, C≡N, NO_2) substituents in the para position are chosen to modulate the basicity of the P-atom in a wider range for studying its effect on the strength and nature of the complexes forming through halogen bonding. The first part of the work deals with the discussion on the geometric and the electronic properties of the chlorine-shared halogen-bonded complexes, whereas the second part deals with the π−halogen-bonded complexes between PPBZ and ClF molecule. In the last part, the variation in the ClF bond distances and ν(Cl−F) stretching vibrations along with C−H bond and ν(CH) stretching vibrations is discussed.

RESULTS AND DISCUSSION

Properties of the Interacting Molecules. In the first step, we discuss the basic properties of the substituted PPBZ and the ClF molecule. Table 1 lists the proton affinity (PA), ionization potential (IP), and the minimum molecular electrostatic potential (MEP) values ($V_{s,min}$) of the substituted PPBZ. The calculated PA value of 814.5 kJ mol^{-1} for C_5H_5P is in good agreement with the experimental value of 817.7 kJ mol^{-1}.[41] As expected, the PA values increases for the $-CH_3$- and $-NH_2$-substituted PPBZ, whereas it decreases for the −F, −CN, and $-NO_2$ substituents. The IP of PPBZis calculated to be 10.03 eV which is in reasonable agreement to the experimental value of 9.2 eV.[42] The negative electrostatic potential $V_{s,min}$ for the XC_5H_4P electron donors were computed from the electron density at the MP2/aug-cc-pVTZ level. The negative electrostatic potential ($V_{s,min}$) on the P atom for the substituted PPBZ are listed in Table 1. The $V_{s,min}$ values on the P atom ranges between −28.16 and −102.22 kJ mol^{-1}. On substitution of EDG, the $V_{s,min}$ values for the $-CH_3$- and $-NH_2$- substituted PPBZ increases by 7.78 and 19.96 kJ mol^{-1}, respectively, indicating a noticeable increase in negative electrostatic potential as compared to C_5H_5P. On the other hand, substitution by EWG leads to a decrease in $V_{s,min}$ by 12.93, 47.11, and 54.10 kJ mol^{-1} for the −F-, −CN-, and $-NO_2$-substituted PPBZ. This result suggests that the $V_{s,min}$ is more sensitive to the EWG substitution. The $V_{s,max}$ on the Cl atom of the ClF molecule has been calculated and predicted to be 211.2 kJ mol^{-1}.

T1-X-PPBZ·ClF Complexes. The schematic representation of the T1-X-PPBZ·ClF (X = NH_2, CH_3, H, F, CN, and NO_2) complexes is shown in Figure 1. The binding energies of the complexes along with other relevant properties are listed in Table 1. As shown in Table S1 of Supporting Information, the intermolecular P···Cl distances (R_1) for all the complexes are found to vary between 2.150 (PPBZ·ClF) and 2.172 Å (F-PPBZ·ClF). This P···Cl distance is almost 1.5 Å less than the sum of the van der Waals radii of P and Cl atoms (3.6 Å), indicating the formation of a strong complex. This observation is in good agreement with a recent study on the H_2XP·ClF (X = OH, CH_3, F, CCH, Cl, H, NC, CN) complexes formed

https://dx.doi.org/10.1021/acsomega.0c03567
ACS Omega 2020, 5, 24095−24105

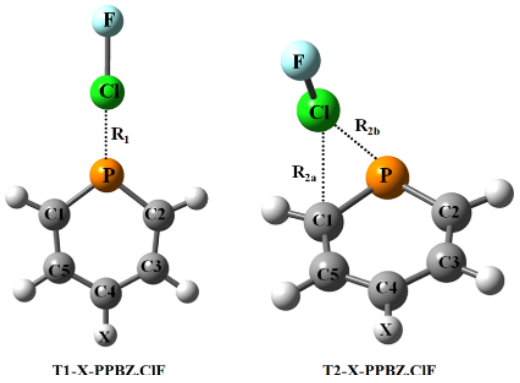

Figure 1. Schematic representation of the two types of complexes formed between PPBZ and ClF.

through the chlorine-shared halogen bond, where the P···Cl distances were found to range between 2.054 and 2.218 Å, almost 1.4−1.5 Å smaller than the sum of the van der Waals radii of P and Cl atoms.[19] For the T1-X-PPBZ·ClF complexes, the PClF bond angle is very close to 180°, indicating that the complexes are perfectly linear. Alkorta et al. predicted the formation of $H_2XP{\cdot}ClF$ complexes as a three-step process in which the first step deals with the dissociation of the ClF molecule into Cl^+ and F^-, the second step leads to the formation of the H_2XPCl^+ cation, and the third step involves the interaction of the H_2XPCl^+ cation with F^- anion.[19] To explore the possibility of the heterolytic cleavage of the ClF bond to Cl^+ and F^- in the presence of PPBZ, we checked the charge polarization of the ClF molecule at several P···Cl distances (*e.g.*, 4.0, 3.0, and 2.5 Å) and by placing the ClF molecule along the C2 axis in the molecular plane by using the MP2/aug-cc-pVDZ method. We have observed that the closer the Cl-atom is to the P-atom, the positive charge on the Cl-atom reduces and negative charge on the F-atom slightly increases, but it does not indicate any cleavage of the Cl−F bond. In fact, the Cl−F bond is found to be elongated by 0.2−6.6% only while changing the P···Cl distance from 4.0 to 2.5 Å. Therefore, the three-step mechanism proposed by Alkorta[19] could not be confirmed from this analysis in this case of the chlorine-shared halogen bond. However, natural bond orbital (NBO) analysis (discussed later) do indicate the interaction between $X{-}C_5H_4PCl^+$ and F^- in the PPBZ·ClF complex. A potential energy scan was also performed by changing the P···Cl distance but keeping the P···F distance fixed at the optimized value of the complex (4.1272 Å). The nature of this curve (as shown in Figure 2) clearly indicates that the chlorine

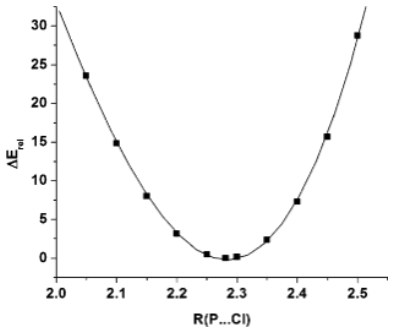

Figure 2. Potential energy profile of the PPBZ−ClF complex.

atom oscillates in a harmonic potential between the P and F atoms, indicating the formation of a chlorine-shared bond between the P, Cl, and the F atoms. The P−Cl distance in the PCl_3 molecule (optimized at MP2 = full/aug-cc-pVTZ level) is found to be 2.045 Å. Therefore, the P···Cl distance in the PPBZ·ClF complexes is just 5−6% higher than the normal covalent P−Cl bond distance, indicating the presence of strong P···Cl interaction in the complex formation between PPBZ and ClF. On complex formation, the Cl−F bond gets elongated by 12−13% as compared to the bond distance of the isolated ClF molecule.

As shown in Table 1, the calculated binding energy values lie between −26.79 and −42.12 kJ mol^{-1}, indicating a wide modulation of the halogen bond strength with the change in the basicity of P in PPBZs. Alkorta et al. in their work on halogen-bonded complexes reported a binding energy ranging between −4.80 and −27.84 kJ mol^{-1} for the FCl·PCX complexes (X = NC, CN, F, H, CH, CCF, CH_3, Li, Na).[17] The calculated binding energy of the $C_5H_5P{\cdot}ClF$ system (−39.43 kJ mol^{-1}) is found to be much higher than the binding energy values for the FCl···PCX systems. It should be noted here that the interaction between PPBZ and Cl_2 molecule calculated at the MP2/aug-cc-pVTZ level results in a traditional halogen-bonded complex with a binding strength of −11.23 kJ mol^{-1} and an intermolecular P···Cl distance of 2.8808 Å. In a similar line, the binding strength of the $C_5H_5N{\cdot}ClF$ complex has also been calculated at the MP2/aug-cc-pVTZ level which is predicted to be −56.14 kJ mol^{-1}. The higher binding strength of the $C_5H_5N{\cdot}ClF$ complex (as compared to the $C_5H_5P{\cdot}ClF$ complex) can be accounted from the much higher PA of the pyridine (921.6 kJ mol^{-1}) than PPBZ (815.5 kJ mol^{-1}). Jiao et al. predicted an interaction energy ranging between −7.32 and −25.18 kJ mol^{-1} for the $XH_2P{\cdots}BrF$ complexes (X = OH, CH_3, Br, NO_2, CF_3, CN) calculated at the CCSD(T)/aug-cc-pVTZ level.[15] The binding energy for the present $XC_5H_4P{\cdot}ClF$ complexes is much higher than that of the $XH_2P{\cdot}BrF$ complexes. Interestingly, the binding strength of the PPBZ·ClF complex is much lower than the previously reported binding strength of the PH_3.ClF complex (−51.2 kJ mol^{-1}).[19] This observation will be discussed in the later part of the paper. For the present T1-X-PPBZ·ClF complexes, the binding energy is the highest for the $NH_2{-}C_5H_4P{\cdot}ClF$ complex (−42.12 kJ mol^{-1}), whereas it is the lowest for the $NO_2{-}C_5H_4P{\cdot}ClF$ complex (−26.79 kJ mol^{-1}), thus indicating that the binding energy increases with the insertion of the electron donating group, whereas it decreases with the inclusion of the electron-withdrawing group. It should be noted that the substitution of $-NH_2$ and $-CH_3$ groups on the C_5H_5P molecule leads to a slight increase of the binding energy (approximately by 2−3 kJ mol^{-1}), but on substitution of −F, −CN and $-NO_2$ groups in the same molecules lead to a noticeable decrease in the binding strength of the complexes. For example, as compared to the binding energy of the $C_5H_5P{\cdot}ClF$ complex, the binding energy increases by 1.66 and 2.69 kJ mol^{-1} for the $-CH_3$ and $-NH_2$ substituted complex, whereas it decreases by 5.97, 12.02, and 12.64 for the −F-, −CN-, and $-NO_2$-substituted complexes. From the data of Table 1, the following correlation between the binding energies and the PA (kJ mol^{-1}) can be deduced

$$-\Delta E = 0.177\mathrm{PA} - 107.5 \qquad (r^2 = 0.930) \tag{1}$$

https://dx.doi.org/10.1021/acsomega.0c03567
ACS Omega 2020, 5, 24095−24105

Table 2. Various Topological Parameters Obtained from AIM Analysis[a]

systems	$\rho(r_c)$	$\nabla^2\rho(r_c)$	$V(r_c)$	$G(r_c)$	$H(r_c)$	$G(r_c)/\rho(r_c)$
			T1-X-PPBZ·ClF			
X = NH_2	0.1137	−0.0460	−0.1065	0.0527	−0.0538	0.4635
CH_3	0.1241	−0.0465	−0.1121	0.0502	−0.0619	0.4045
H	0.1243	−0.0453	−0.1127	0.0507	−0.062	0.4078
F	0.1176	−0.0217	−0.1061	0.0503	−0.0558	0.4277
CN	0.1184	−0.0181	−0.1084	0.0519	−0.0565	0.4383
NO_2	0.1190	−0.0188	−0.1094	0.0524	−0.057	0.4403
			T2-X-PPBZ·ClF			
X = CH_3	0.0245	0.0638	−0.0174	0.0167	−0.0007	0.6816
H	0.0234	0.0629	−0.0168	0.0163	−0.0005	0.6966
F	0.0223	0.0588	−0.0149	0.0148	−0.0004	0.6637
CN	0.0202	0.0585	−0.0142	0.0144	0.0002	0.7129
NO_2	0.0200	0.0587	−0.0142	0.0145	0.0003	0.7250

[a]Values are in a.u.

The changes in the standard Gibbs free energies (ΔG) for all the complexes at 298 K temperature are calculated at the MP2/aug-cc-pVTZ level. These calculated ΔG values can be useful in estimating the thermodynamic stability of the complexes and in speculating whether these complexes can exist at room temperature. The negative ΔG value ranging between −6.24 and −21.62 kJ mol^{-1} suggests that these T1-X-PPBZ·ClFcomplexes can be formed spontaneously and likely to be found by experimental techniques at room temperature. It should be noted that the increase in the negative ΔG values parallels with the increase in the binding strength of the complexes.

As established in many recent works, the electrostatic potential $V(r)$ can be used as an important property for measuring the strength of σ-hole and also in explaining and predicting the nature and strength of various noncovalent interactions. In similar line, it may be interesting to find whether the minimum value of $V(r)$ ($V_{s,min}$) on the P-atom of PPBZ can also be used to measure the strength of the interaction. The $V_{s,min}$ values of the substituted PPBZs are listed in Table 1. It should be noted that $-NH_2$-substituted PPBZ having the maximum $V_{s,min}$ value (−102.22 kJ mol^{-1}) is characterized by the highest binding energy, whereas the $-NO_2$-substituted PPBZ possessing the least $V_{s,min}$ value (−28.16 kJ mol^{-1}) is characterized by a lowest binding energy. In several studies on halogen-bonding interactions, a linear correlation between the binding energy of the halogen bonded complex and the magnitude of the negative electrostatic potential ($V_{s,min}$) has been established. The same correlation holds good for our present study as well. The interaction energies (kJ mol^{-1}) are linearly related to the $V_{s,min}$ of the substituted PPBZ by the relations

$$-\Delta E = -0.224V_{s,min} + 19.83 \qquad (r^2 = 0.969) \qquad (2)$$

In order to understand the nature of the P···Cl bond, we have further carried out the atom-in-molecule (AIM) analysis for all the XC_5H_5P·ClF complexes. Several topological parameters such as bond critical points (BCP) and analysis of various properties at BCP, like electron density $\rho(r_c)$, its Laplacian $[\nabla^2\rho(r_c)]$ and total local energy $H(r_c)$, which are capable of providing important information about the nature of bonding, are listed in Table 2. As shown in Figure 3, AIM analysis shows the existence of a BCP between the Cl and P atoms in the C_5H_5P·ClF complex. The bond path length between P and Cl atoms found from the AIM analysis is exactly the same as obtained from the MP2 optimized geometry, indicating that the bond path is not bent and leads directly between the two atoms. The existence of the BCP between the Cl and P atoms along with a linear bond path has been observed for the other complexes as well.

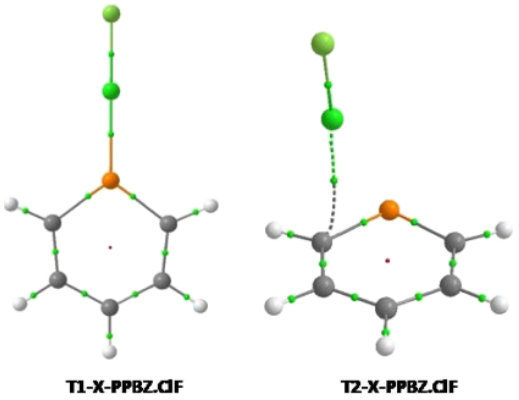

Figure 3. Existence of BCP's in T1-X-PPBZ·ClF and T2-X-PPBZ complexes.

The $\rho(r_c)$ values at the BCP of the P···Cl bond for the T1-X-PPBZ·ClF complexes are found to range between 0.1137 and 0.1243 a.u. These values are quite high compared to the values observed for the traditional halogen bond and are in good agreement with the $\rho(r_c)$ values (ranging between 0.0270 and 0.1224 a.u.) of the recently studied halogen-bonded complexes between PH_2X with BrCl and BrF.[15] The $\rho(r_c)$ value for a pure covalent P−Cl bond in PCl_3 is found to be 0.1317 a.u., indicating that the P···Cl bond in T1-X-PPBZ·ClF complexes is highly covalent in nature. In various recent works on noncovalent interactions, $H(r_c)$ and the ratio $G(r_c)/\rho(r_c)$ were used as indicators in predicting whether an interaction is predominantly covalent or electrostatic.[43,44] For the same complexes between PH_2X with BrCl and BrF, the $H(r_c)$ values were found to be all negative ranging between −0.0188 and −0.1452 a.u., indicating the presence of partial covalent character.[15] Similarly, for the T1-X-PPBZ·ClF complexes, the $H(r_c)$ values are found to be negative, ranging between −0.0538 and −0.062 a.u. Moreover, the values of ratio $G(r_c)/\rho(r_c)$ are less than 1 for all the complexes. These results suggest that the P···Cl bonded complexes have a significant covalent character. It should be noted the $\rho(r_c)$ values at the BCP of

https://dx.doi.org/10.1021/acsomega.0c03567
ACS Omega 2020, 5, 24095−24105

Table 3. Charges, q(e) of Cl and F in ClF and P in X-PPBZ-ClF Complexes, Intermolecular CT (in e), % s Character of Cl in ClF Molecule, and Second-Order Hyperconjugation Energy (in kJ mol^{-1})[a,b]

	ClF					
systems	q(Cl)	q(F)	q(P)	CT	% s (Cl)	LP(F) → σ^*(PCl)
			T1-X-PPBZ·ClF			
X = NH_2	0.0880	−0.5957	0.9665 (0.5792)	0.5077		638.81
CH_3	0.0902	−0.5974	1.0291 (0.6342)	0.5072		630.11
H	0.0930	−0.5950	1.0445 (0.6526)	0.5020		636.18
F	0.1028	−0.5767	0.9929 (0.6350)	0.4739		698.73
CN	0.1154	−0.5677	1.0513 (0.7041)	0.4523		714.79
NO_2	0.1169	−0.5678	1.0622 (0.7163)	0.4509		711.99
	ClF					
systems	q(Cl)	q(F)	q(P)	CT	% s (Cl)	σ(C1P) → σ^*(ClF)
			T2-X-PPBZ·ClF			
X = CH_3	0.3104	−0.3912	0.6778	0.0808	4.71	83.30
H	0.3168	−0.3861	0.6951	0.0693	4.80	73.30
F	0.3111	−0.3839	0.6593	0.0728	4.93	72.76
CN	0.3253	−0.3711	0.7336	0.0458	5.27	53.97
NO_2	0.3272	−0.3695	0.7482	0.0423	5.32	

[a]Values in parenthesis indicate the charges (e) on P in isolated PPBZs. [b]In isolated ClF, q(Cl) = 0.353 e and q(F) = −0.353 e.

Cl−F bond are found to range between 0.1272 and 0.1358 a.u., whereas the $\nabla^2\rho(r_c)$ values are found to range between 0.1525 and 0.2130 a.u. Unlike the P−Cl bond and other covalent bonds, $\nabla^2\rho(r_c)$ values the for the Cl−F bond are all significantly positive, indicating the validity of X−$C_5H_4PCl^+$ and F^- type of interaction in the T1-PPBZ-ClF complexes.

We like to note here that the symmetry-adapted perturbation theory (SAPT) calculations could not be performed for these T1-X-PPBZ·ClF complexes.

From NBO analysis, first, we have calculated the amount of CT in the present para-substituted X−C_5H_4P·ClF complexes. Table 3 lists the values of the CT along with the net atomic charges on the Cl, F, and P atoms obtained from the natural population analysis (NPA) and second-order hyperconjugation energies. The CT values are quite high and range between 0.4509 and 0.5077 e. The binding energy of the T1-X-PPBZ·ClF complexes (kJ mol^{-1}) is linearly correlated to the intermolecular CT (e).

$$-\Delta E = 254.07\mathrm{CT} - 87.49 \qquad (r^2 = 0.995) \qquad (3)$$

The net atomic charge on the P atom in isolated PPBZ molecules was found to be positive and varies within a range of 0.5792−0.7163 e. Apparently, the positive charge on the P-atom of PPBZ does not commensurate well with the negative MEP value on the P-atom. In this context, we like to highlight that the MEP value corresponds to the electron density distribution of the whole molecule, whereas atomic charge is estimated in a localized center following semi-empirical prescriptions. The net atomic charge obtained from the Mulliken analysis and electrostatic potential-driven method (ChelPG) is found to be negative for the P-atom of isolated PPBZ and becomes positive on complex formation. However, the most important point to note is the trend of change in atomic charge while going from the isolated monomer to the complex remaining the same for all the methods. Similar observation was also made for the CT values, where the variation of CT with the change in substituent in PPBZ does not depend much on the method of calculating atomic charge. Therefore, NPA charges are given in Table 3 for consistency with our NBO analysis and the atomic charges obtained from the Mulliken and ESP analysis are given as Supporting Information in Table S2. Complex formation leads to a further decrease in the electron density on P ranging between 0.3873 e (NH_2−C_5H_4P·ClF) and 0.3459 e (NO_2−C_5H_4P·ClF) in all the complexes. A significant variation of the charges is predicted for the Cl and F atom of the ClF molecule in the T1-X-PPBZ·ClF complexes. In the isolated ClF molecule, the valence 3s, $3p_x$, $3p_y$, and $3p_z$ orbital occupancies of the Cl atom are 1.9263, 1.9982, 1.9982, and 0.6918 e, respectively (shown in Table S3 of Supporting Information). These values indicate that the $3p_z$ orbital has the electron depleted area (σ-hole) which eventually interacts with a lone pair of P (of PPBZ) to form the halogen bond. It should be noted that on complex formation, the $3p_z$ orbital occupation increases sharply ranging between 1.917 e (NO_2-PPBZ·ClF) and 1.936 e (NH_2-PPBZ·ClF), indicating a noticeable electron transfer from the lone pair of P to the $3p_z$ orbital of Cl. NBO analysis indicates the formation of a covalent bond from the overlap of a sp^2 orbital of P atom and the p_z orbital of the Cl atom with σ(P−Cl) occupation of above 1.93 e, whereas no σ(Cl−F) orbital is found from this analysis. It indicates that in T1-X-PPBZ·ClF complexes, there is an ion-pair interaction between X−C_5H_4P·Cl^+ and F^-, which supports the mechanism proposed by Alkorta et al.[19] The NBO analysis reveals the existence of a strong LP(F) → σ^*(P−Cl) hyperconjugation interaction in the T1-PPBZ·ClF complexes (as shown in Table 3) instead of LP(P) to σ^*(Cl−F) hyperconjugation, which is generally observed in the traditional P···Cl halogen bond. It clearly shows the contrasting behavior of chlorine-shared and traditional halogen bonds.

As indicated in Table 3, the positive charge on the Cl atom decreases, whereas the negative charge on the F atom increases upon complex formation. It should be noted that this decrease in the positive charge of Cl and increase in the negative charge on the F atom in the ClF molecule parallels with the increase in the binding strength of the complexes. NBO calculation further reveals the formation of the σ(P−Cl) orbital in PPBZ·ClF complexes, indicating the higher strength and significant covalent nature of the P···Cl bond in T1-X-PPBZ·ClF complexes. The σ(P−Cl) bonding population ranges between

https://dx.doi.org/10.1021/acsomega.0c03567
ACS Omega 2020, 5, 24095−24105

1.9539 and 1.9578 e, whereas σ^*(P−Cl) antibond population varies between 0.3390 and 0.3600 e for T1-PPBZ·ClF complexes. A bond order of 0.8 has been predicted for the P···Cl bond in all the complexes. Let us now try to explain the variation of P···Cl distances in terms of σ^*(P−Cl) antibond occupation and LP(F) → σ^*(P−Cl) hyperconjugation energy. As indicated in Table 4, for the stronger complexes, the σ^*(P−Cl) population is low, whereas it is slightly higher for the weaker complexes. The hyperconjugation energies LP(F) → σ^*(P−Cl) range between 630.1 and 714.8 kJ mol^{-1}. Contrary to our normal expectation, complex with the highest $E^{(2)}$ values are characterized with the lowest P···Cl binding strength and *vice versa*. This is quite opposite to the trends obtained in many of the recent studies on traditional halogen-bonded complexes (both closed shell and open shell), where higher hyperconjugation energy is associated with higher stability of the complexes.[23,45] One possibility is that the energy difference of the lone pair of fluorine and the antibonding orbital of Cl−F bond increases with the lengthening of the Cl−F bond, making it difficult for the CT. Therefore, the complex with the highest binding energy is associated with highest lengthening of the Cl−F bond, and consequently, lower hyperconjugation energy has been observed. Further, this result is well complimented by the higher P···Cl intermolecular distances in the weaker complexes. In fact, the P···Cl distance is the result of a competition between two interactions: (i) the covalent interaction between orbitals of P and Cl trying to reduce the P···Cl distance and (ii) the LP(F) → σ^*(P−Cl) hyperconjugation interaction effecting a lengthening of the P···Cl distance. As a result, there is very little variation in P···Cl distance (only 0.02 Å) in spite of a large variation of binding energy (∼15 kJ mol^{-1}) for the T1-X-PPBZ·ClF complexes.

Table 4. Variation in Bond Distance, Δr(Cl−F) in mÅ, Stretching Frequency $\Delta\nu$(Cl−F) and ν(P−Cl) in cm^{-1}, Antibonding Occupation, σ^*(P−Cl) and σ^*(Cl−F) in e[a]

system	Δr(Cl−F)	$\Delta\nu$(Cl−F)	σ^*(P−Cl)	ν(P−Cl)
		T1-X-PPBZ·ClF		
X = NH_2	+216.6	−327	0.3390	459
CH_3	+217.4	−326	0.3364	455
H	+215.3	−325	0.3383	499
F	+200.3	−314	0.3547	450
CN	+193.5	−309	0.3600	416
NO_2	+194.4	−311	0.3595	386
system	Δr(Cl−F)	$\Delta\nu$(Cl−F)	σ^*(Cl−F)	ν(P−Cl)
		T2-X-PPBZ·ClF		
X = CH_3	+37.1	−117	0.0960	
H	+32.3	−105	0.0841	
F	+31.6	−105	0.0873	
CN	+22.0	−76	0.0621	
NO_2	+20.7	−72	0.0585	

[a]In isolated ClF: r(Cl−F): 1.6346 Å and ν(Cl−F): 806 cm^{-1}.

These results suggest that the LP(F) → σ^*(P−Cl) hyperconjugation cannot be taken as the only parameter in determining the stability of the these complexes rather parameters like $V_{s,min}/V_{s,max}$, IP, and intermolecular CT are more important in predicting the stability of these complexes. It should be noted that in all isolated substituted PPBZs, the lone pair of P is involved in LP(P) → σ^*(C1C2) and LP(P) → σ^*(C4C5) hyperconjugation. However, on complex formation, these orbital interactions are observed only for −NH_2-and −CH_3-substituted complexes. For the NH_2-Phos-ClF complex, the LP(P) → σ^*(C1C2) and LP(P) → σ^*(C4C5) value amounts to 234 kJ mol^{-1} each, whereas, for the CH_3-Phos-ClF complex, it amounts to 196 and 474 kJ mol^{-1}. This increase in the hyperconjugation energy in −NH_2- and −CH_3-substituted complexes can be the reason for the higher stability of these complexes than other substituted complexes.

There is a sharp difference in the orbital interaction in pyridine·ClF and PPBZ·ClF complexes. For example, in pyridine·ClF complexes, there is no LP(F) → σ^*(N−Cl) hyperconjugation interaction even though the binding energy is quite high, but there is strong LP(N) → σ^*(Cl−F) interaction. On the other hand, PPBZ·ClF complexes are characterized with strong LP(F) → σ^*(P−Cl) interaction and no LP(P) → σ^*(Cl−F) interaction. Various previous studies on chlorine-shared halogen bonded complexes also satisfy these criteria. Perhaps this difference of interaction can be used as an indication of the formation of a chlorine-shared bond.

Comparison between N-Base Complexes and P-Base Complexes. In order to have a better knowledge on the strange nature of the P···Cl bonded complexes, a comparative analysis has been carried out at the MP2/aug-cc-pVTZ level, taking pyridine, NH_3, PPBZ, and PH_3 as electron donors and ClF as the electron acceptor. As indicated in Table 5, the binding energies of the complexes containing NH_3, pyridine, PH_3, and PPBZ are found to be −35.70, −56.14, −33.84, and −39.43 kJ mol^{-1}, respectively. Let us note that the binding strength of the complexes containing N···Cl and P···Cl bond increases with the increase in the PA value of the electron donor N/P atom, but there is no general correlation for them together. Similar observation can be made from the IP value as well. The most important difference between the complexes

Table 5. Various Properties of NH_3, PH_3, Pyridine, PPBZ, and Their Complexes with ClF Molecule[a]

parameters	NH_3−ClF	pyridine−ClF	PH_3−ClF	PPBZ−ClF
PA (kJ mol^{-1})	853.6	930.0	785.0	817.7
IP (eV)	10.02	9.34	9.87	9.2
P···Cl/N···Cl	2.2068	2.0469	2.1637	2.150
r(ClF) (Å)	1.7133	1.7536	1.8484	1.8499
ΔE (kJ mol^{-1})	−35.70	−56.14	−33.84	−39.43
ΔG (kJ mol^{-1})	−10.38	−30.18	−13.28	−18.74
CT (e)	0.2065	0.2542	0.5319	0.5020
q(N)/q(P) (e)	−0.9437 (−1.0539)	−0.3899 (−0.4287)	0.4810 (0.0286)	1.0445 (0.6526)
LP(N) → σ^*(ClF)/LP(F) → σ^*(PCl) (kJ mol^{-1})	250.47	392.79	674.86	636.18

[a]Values in parenthesis indicate the charge for the isolated molecule. T2-X-PPBZ·ClF complexes.

https://dx.doi.org/10.1021/acsomega.0c03567
ACS Omega 2020, 5, 24095−24105

containing the N···Cl and the P···Cl bond is the mode of hyperconjugation. In halogen-bonded complex with N-bases, the system is stabilized by LP(N) → σ*(ClF) interaction, whereas for complexes with the P-base, there is a bond formation with the overlap of a sp^2 orbital of P atom and the p_z orbital of Cl. The P-base complexes are further stabilized by a strong LP(F) → σ*(PCl) hyperconjugation. The CT is found to be much higher for the P-base complex in comparison to the corresponding N-base complex.

T2-X-PPBZ.ClF Complexes. The schematic representation of the geometries of the T2-X-PPBZ·ClF complexes between PPBZ and ClF is shown in Figure 1. These complexes are formed by the interaction of the ClF molecule with the π-electron cloud of the C1═P double bond. The ClF molecule in these complexes lies almost perpendicular to the aromatic ring and the acidic Cl atom is oriented toward the π-bond between C1 and P of the PPBZ molecule. The structure of the NH_2−C_5H_4P·ClF π-complex could not be obtained as during optimization it always goes to the geometry of the T1-complex with the chlorine-shared halogen bond. As cited in Table S1 of Supporting Information, the C1···Cl distance (R_{2a}) in these complexes ranges between 2.731 and 2.810 Å, whereas P···Cl distances (R_{2b}) vary between 2.990 and 3.136 Å. As shown in Figure 3, one BCP between the Cl atom and the C1 atoms in ortho position is predicted for the T2-X-PPBZ·ClF complexes. In T2 complexes, as compared to the monomer units, both C1−P and ClF bonds get elongated on complex formation. The C1−P bond elongation varies between 6 and 8.2 mÅ. The MP2-calculated binding energy of these complexes varies between −14.75 and −20.54 kJ mol^{-1}. In comparison to the chlorine-shared halogen bond, here, the variation in binding energy is quite less and lies within 6 kJ mol^{-1}. As expected, the binding strength is the highest for the CH_3−C_5H_4P·ClF complex, whereas it is the lowest for the NO_2−C_5H_4P·ClF complex. Unlike T1-X-PPBZ·ClFcomplexes, T2-X-PPBZ·ClF complexes are all characterized by positive Δ*G* values, which is the direct reflection of the lower binding strength of the T2-X-PPBZ·ClF complexes.

AIM analysis shows a small variation in the $\rho(r_c)$ values ranging between 0.020 and 0.0245 a.u. for the T2-X-PPBZ·ClF complexes. These $\rho(r_c)$ values are all within the range proposed by Popelier,[46] which confirms the formation of these complexes through π−halogen interaction rather than through weak van der Waals interactions. The binding strength of the T2-X-PPBZ·ClF complexes are found to correlate linearly with the $\rho(r_c)$ values at BCP

$$-\Delta E = 1220\rho(r_c) - 9.609 \qquad (r^2 = 0.987) \tag{4}$$

The $H(r_c)$ value for the complexes containing $-CH_3$, −H, and −F are found to be negative, whereas it becomes positive for the −CN- and $-NO_2$-substituted complexes. The negative $H(r_c)$ values are quite low which reflects that these complexes are predominantly electrostatic in nature. These values are in agreement with the lower binding strength of the T2-X-PPBZ·ClF complexes.

Table 6 reports the various important energetic components for the halogen-bonded complexes calculated at SAPT2+/aug-cc-pVTZ level. It should be noted that the halogen-π complexes between pyridine and XY dihalogen molecules were purely dominated by induction energy.[37] Our calculation shows that for the C_5H_5P·ClF complex, 37% of the total attraction energy is because of classical electrostatic energy and 29% because of induction energy, whereas dispersion energy contributes up to 31% of the total attraction energy. This result suggests that unlike pyridine−XY complexes,[37] the PPBZ−ClF complex is dominated by electrostatic attraction. On substitution of EDG, only the electrostatic contribution increases to a noticeable change. On the other hand, for −CN- and NO_2-substituted complexes, the dispersion energy contribution overpowers the electrostatic energy. The variation of the induction energy with the change in the substituent in PPBZ is found to be very small. It may be mentioned here that the small difference between the binding energy reported in Table 1 and the SAPT interaction energy is because of the deformation energy as in SAPT monomer energy is computed for the distorted structure within the complex and also for the inclusion of higher-order electron correlation in SAPT.

Table 6. Results of SAPT Analysis Using the aug-cc-pVTZ Basis Set[a]

systems	ΔE_{elst}	ΔE_{exch}	ΔE_{ind}	ΔE_{disp}	ΔE_{int}^{SAPT}
			T2-X-PPBZ·ClF		
X = CH_3	−51.91 (38.8)	116.67	−40.39 (30.2)	−41.52 (31.0)	−17.15
H	−47.16 (36.9)	107.08	−36.42 (28.5)	−39.20 (30.7)	−15.70
F	−44.16 (37.3)	104.24	−35.60 (30.1)	−38.58 (32.6)	−14.10
CN	−35.28 (35.3)	87.93	−28.17 (28.2)	−36.56 (36.6)	−12.09
NO_2	−34.15 (35.1)	85.24	−27.14 (27.9)	−36.16 (37.1)	−12.20

[a]Data are in kJ mol^{-1}. Values in the parenthesis indicate % contribution of electrostatic, induction, and dispersion term in total attractive interaction.

The CT values for the present complexes are found to range between 0.0426 and 0.0807 e. The strongest complex (CH_3−C_5H_4P·ClF) is characterized by the highest CT, whereas the CT decreases in the weaker complexes. The binding energies (kJ mol^{-1}) of the halogen−π bonded complexes are linearly correlated to the intermolecular CT (e).

$$-\Delta E = 139.9\mathrm{CT} + 8.639 \qquad (r^2 = 0.967) \tag{5}$$

Moreover, this CT (me) is found to be correlated to the negative electrostatic potential (kJ mol^{-1}) of the PPBZ and can be expressed as

$$\mathrm{CT} = -0.607V_{s,min} + 25.20 \qquad (r^2 = 0.991) \tag{6}$$

For T2-X-PPBZ·ClF complexes, the positive charge on Cl decreases and the negative charge on F increases in comparison to the charges in the isolated ClF molecule. The strongest π-complex is characterized by the highest decrease in the positive charge on the Cl atom and the maximum increase in the negative charge of the F atom. It is also interesting to compare the % *s* character of the Cl in isolated ClF with that of the complexes. Moreover, the applicability of the Bent's rule[47] can be tested here for the T2-X-PPBZ·ClF complexes from a correlation between the % *s* character of the Cl atom and the negative charge on the F atom. Table 3 indicates that the negative charge on the F atom increases with the increase in strength of the T2-X-PPBZ·ClF complexes. This increase leads to a decrease in the s-character of the Cl atom which takes a value ranging between 4.71 and 5.32%. A linear correlation between % *s* character of Cl and *q*(F) has been obtained below

$$\%\, s\ (\mathrm{Cl}) = 28.67q(\mathrm{F}) + 15.91 \qquad (r^2 = 0.992) \tag{7}$$

https://dx.doi.org/10.1021/acsomega.0c03567
ACS Omega 2020, 5, 24095−24105

This equation illustrates the validity of the Bent's rule for the T2-X-PPBZ·ClF complexes. A similar correlation was previously obtained for the FDME·ClF complexes[48] with slightly low slope (26.76) and intercept (14.33). There is a slight increase in the positive charge of the P atom on complex formation. The negative charge on C1 increases to some extent, whereas the negative charge on C2 decreases slightly upon complex formation. Wang et al. studied the π−halogen complexes between pyridine and XY (where XY = F, Cl, Br) molecules in which they have predicted that the CT mainly takes place from the C1C2 bond of the pyridine to the XY antibonding orbital.[35] However, for the present T2-X-PPBZ·ClF complexes, the stability of the halogen−π complexes is mainly because of the σ(C1P) → σ^*(ClF) second-order hyperconjugation energy except for the NO_2-substituted complex, where σ(C1C2) → σ^*(ClF) was found to be the dominating factor. The σ(C1P) → σ^*(ClF) hyperconjugation energy for the $-CH_3$-, −H-, −F-, and −CN-substituted complexes are found to be 83.3, 73.3, 72.8, and 54 kJ mol^{-1}. The increase in the hyperconjugation energy parallels with the increase in the binding strength of the complexes. For the $-NO_2$ substituted complex, a low value of 6.48 kJ mol^{-1} has been predicted for the σ(C1C2) → σ^*(ClF) hyperconjugation energy.

Variation in *r*(Cl−F) Bond Distance and ν(Cl−F) Stretching Vibration. In this section, we will discuss the elongation of the ClF molecule and the redshift of the ν(Cl−F) stretching vibrational frequencies of both T1-X-PPBZ·ClF and T2-X-PPBZ·ClF complexes. For the T1-X-PPBZ·ClF complexes, the Cl−F bond distance [r(Cl−F)] increases substantially ranging between 193.5 and 216.6 mÅ which results in the redshift of the ν(Cl−F) stretching vibration ranging between 309 and 327 cm^{-1}. The elongation as well as the redshift is the largest for the $-CH_3$- and $-NH_2$-substituted complex, whereas it decreases in the weaker complexes. For the linear complexes, the decrease in the ν(Cl−F) stretching vibrations is linearly correlated with the elongation of the r(ClF) bond distance (in mÅ) by this equation

$$\Delta\nu(\mathrm{ClF}) = -0.71\Delta r(\mathrm{ClF}) - 170.8 \qquad (r^2 = 0.992) \tag{8}$$

A smaller elongation ranging between 20.7 and 37.1 mÅ and a redshift between 72 and 117 cm^{-1} are predicted for the T2-X-PPBZ·ClF complexes. A linear correlation between the variation in ν(Cl−F) stretching vibrations and elongation of the r(ClF) bond can be obtained for the T2-X-PPBZ·ClF complexes as well.

$$\Delta\nu(\mathrm{ClF}) = -0.356\Delta r(\mathrm{ClF}) - 5.125 \qquad (r^2 = 0.996) \tag{9}$$

As indicated in Table 4, for T2-X-PPBZ·ClF complexes, there is an increase in the occupation of the antibonding σ^*(ClF) orbital of the electron acceptor ClF molecule. The σ^*(ClF) occupation for these complexes varies from 0.0585 and 0.0960 e. For the present P···Cl-bonded complexes, the elongations are linearly related to σ^*(ClF) occupation (r in mÅ, σ^* occupation in e)

$$\Delta r(\mathrm{ClF}) = 428.4\sigma^*(\mathrm{ClF}) - 4.51 \qquad (r^2 = 0.987) \tag{10}$$

As the electron occupation of the bonding σ(ClF) orbital remains constant, it can be concluded from this equation that the increase in the antibonding σ^*(ClF) occupation is responsible for the elongation of the r(ClF) bond distances upon complex formation.

A linear correlation between interaction energies and the frequency shifts of the ν(AH) stretching vibrations (originally known as the Badger−Bauer relation)[49] has been established for several hydrogen-bonded and halogen-bonded complexes. For the present systems, we have also obtained a similar correlation which can be written as

$$-\Delta E = -0.816\Delta\nu(\mathrm{ClF}) - 225.2 \qquad (r^2 = 0.958)\ (\text{T1-X-PPBZ. ClF complexes}) \tag{11}$$

$$-\Delta E = -0.119\Delta\nu(\mathrm{ClF}) + 5.979 \qquad (r^2 = 0.962)\ (\text{T2-X-PPBZ. ClF complexes}) \tag{12}$$

As shown in Table 4, the intermolecular ν(P−Cl) stretching vibrations are predicted at higher wavenumbers for the complexes involving the electron-donating substituent at PPBZ. The ν(P−Cl) vibrations are predicted at 459, 455, and 499 cm^{-1} for $-NH_2$-, $-CH_3$-, and −H-substituted complexes and 450, 416, and 386 cm^{-1} for the −F-, −CN-, and $-NO_2$-substituted complexes, respectively. As expected, these values are lower than the experimental gas-phase ν(P−Cl) value of 504 cm^{-1} for the P−Cl covalent bond in PCl_3, but their magnitude certainly indicates the formation of a relatively strong covalent P−Cl bond in T1-complexes.

It has been discussed in several recent works that the interaction between FDME and the dihalogen molecule (ClF, Cl_2, *etc.*) results in variation of the CH bond lengths.[48] Moreover, interaction of pyridine with the Cl^0 atom results in a shortening of the ortho CH bond by 0.8 and 1.6 mÅ, and consequently, a blue shift in ν(CH) stretching vibration ranging between 19 and 27 cm^{-1} has been predicted.[50] Therefore, it seemed interesting to investigate the changes of CH bond lengths in the present complexes as well. For T1-X-PPBZ·ClF complexes, the contraction of the $C1H_0$ bonds ranges between 1.4 and 1.9 mÅ. The contraction of the other CH bonds is much smaller between 0.2 and 0.9 mÅ but is systematically predicted in all the complexes. A very negligible amount of changes has been observed for the ν(CH) stretching vibration in T1-X-PPBZ·ClF complexes. A similar trend and almost no change in CH bond length and vibrational frequencies are predicted for the T2-X-PPBZ·ClF complexes as well.

CONCLUSIONS

This present work features the theoretical investigation of the interaction between para-substituted PPBZ (XC_5H_4P, X = H, $-NH_2$, $-CH_3$, −F, −CN, $-NO_2$) and ClF molecule. The calculations were carried out using the *ab initio* MP2(full)/aug-cc-pVTZ method. The main conclusions of this work are as follows:

1. T1-X-PPBZ·ClF complexes formed through the chlorine-shared halogen bond, whereas T2-X-PPBZ·ClF complexes are formed *via* halogen−π interaction.
2. The binding strength of the T1-X-PPBZ·ClF complexes ranging between −42.12 and −26.79 kJ mol^{-1} are much higher than the binding strength of the T2-X-PPBZ·ClF complexes varying between −20.54 and −14.75 kJ mol^{-1}. Moreover, the negative ΔG values of the T1-X-PPBZ·ClF complexes suggest that these complexes can exist in experimental conditions as well.

https://dx.doi.org/10.1021/acsomega.0c03567
ACS Omega 2020, 5, 24095−24105

3. SAPT analysis indicates that the T2-X-PPBZ·ClF complexes are predominantly stabilized by both electrostatic and dispersion energy.
4. AIM and NBO analyses suggest that T1-X-PPBZ·ClF complexes have a covalent character and are stabilized by a Cl-shared halogen bond. The $\rho(r_c)$ value at the BCP of the P···Cl bond and the σ(P−Cl) orbital occupation for the T1-X-PPBZ·ClF complexes are found to be close to the value of a normal P−Cl bond in PCl_3.
5. Complex formation results in the elongation of the ClF bond both in T1-X-PPBZ·ClF and T2-X-PPBZ·ClF complexes, and consequently, a redshift for the ν(ClF) stretching vibration has been observed.

Computational Methodology. The geometries of the para-substituted PPBZ (XC_5H_4P, X = NH_2, CH_3, H, F, CN, NO_2) and its complexes with the ClF molecule were optimized using the *ab initio* MP2 method in conjunction with the aug-cc-pVTZbasis set. Harmonic frequency calculations were carried at the same level in order to characterize the stationary points. The binding energy (ΔE) of the complexes were calculated following the super molecular approach, where the energies of the fully optimized isolated PPBZ and ClF molecules were subtracted from the total energy of the complexes. The binding energy of the complexes includes zero point energy and the basis set superposition error correction computed by the counterpoise method.[51] The IP of the substituted PPBZ and electron affinity of the ClF molecule were calculated at the MP2 = full/aug-cc-pVTZ level. NBO[52] analysis was performed at the wB97XD/aug-cc-pVTZ level on the MP2 optimized geometries, to obtain ideas about the charges on the individual atoms, orbital occupancies, hyperconjugation energies, hybridization, and so forth. AIM[53] analysis was carried out at the MP2/aug-cc-pVTZ level to have a better understanding about the nature of interaction. The electrostatic potential of the isolated substituted PPBZ was calculated at the MP2/aug-cc-pVTZ level using wave function analysis surface analysis suite.[54] The electrostatic potential was computed on 0.001 a.u. isodensity surface. The energy decomposition analysis was carried out employing SAPT using the Psi4 program.[55] All electronic structure calculations were carried out using the G09 suite of program.[56]

■ ASSOCIATED CONTENT

Supporting Information

The Supporting Information is available free of charge at https://pubs.acs.org/doi/10.1021/acsomega.0c03567.

Intermolecular P···Cl distances (R_1) of T1 complexes, C1···Cl (R_{2a}) and P···Cl (R_{2b}) distances of T2 complexes, and valence (3s, $3p_x$, $3p_y$, $3p_z$) orbital occupancies of Cl in isolated ClF and in complexes (PDF)

■ AUTHOR INFORMATION

Corresponding Author

Asit K. Chandra − *Department of Chemistry, North-Eastern Hill University, Shillong 793022, India;* orcid.org/0000-0001-6079-0989; Email: akchandra.bwn@gmail.com

Authors

Dipankar Sutradhar − *Solid State and Structural Chemistry Unit, Indian Institute of Science, Bangalore, Karnataka 560012, India*

Sumitra Bhattarai − *Department of Chemistry, North-Eastern Hill University, Shillong 793022, India*

Salma Parveen − *Department of Chemistry, North-Eastern Hill University, Shillong 793022, India*

Complete contact information is available at: https://pubs.acs.org/10.1021/acsomega.0c03567

Notes

The authors declare no competing financial interest.

■ ACKNOWLEDGMENTS

D.S. thanks CSIR-India and S.B. thanks UGC-India for providing a research fellowship, and A.K.C. thanks Computer Centre, NEHU, and DST, India, for providing computational facilities and financial support. Authors also thank Tirna Chandra (MA, English) for helping in editing the manuscript.

■ REFERENCES

(1) Nguyen, H. L.; Horton, P. N.; Hursthouse, M. B.; Legon, A. C.; Bruce, D. W. Halogen Bonding: A New Interaction for Liquid Crystal Formation. *J. Am. Chem. Soc.* **2004**, *126*, 16−17.

(2) Lauher, J. W.; Fowler, F. W.; Goroff, N. S. Single-Crystal-to-Single-Crystal Topochemical Polymerization by Design. *Acc. Chem. Res.* **2008**, *41*, 1215−1229.

(3) Metrangolo, P.; Meyer, F.; Pilati, T.; Resnati, G.; Terraneo, G. Halogen Bonding in supramolecular Chemistry. *Angew. Chem., Int. Ed.* **2008**, *47*, 6114−6127.

(4) Auffinger, P.; Hays, F. A.; Westhof, E.; Ho, P. S. Halogen bonds in biological molecules. *Proc. Natl. Acad. Sci. U.S.A.* **2004**, *101*, 16789−16794.

(5) Wilcken, R.; Zimmermann, M. O.; Lange, A.; Joerger, A. C.; Boeckler, F. M. Principles and Applications of Halogen Bonding in Medicinal Chemistry and Chemical Biology. *J. Med. Chem.* **2013**, *56*, 1363−1388.

(6) Ford, M. C.; Ho, P. S. Computational Tools To Model Halogen Bonds in Medicinal Chemistry. *J. Med. Chem.* **2016**, *59*, 1655−1670.

(7) Cavallo, G.; Metrangolo, P.; Milani, R.; Pilati, T.; Priimagi, A.; Resnati, G.; Terraneo, G. The Halogen Bond. *Chem. Rev.* **2016**, *116*, 2478−2601.

(8) Clark, T.; Hennemann, M.; Murray, J. S.; Politzer, P. Halogen Bonding: The Sigma-Hole. *J. Mol. Model.* **2007**, *13*, 291−296.

(9) Vogel, L.; Wonner, P.; Huber, S. M. Chalcogen Bonding: An Overview. *Angew. Chem., Int. Ed.* **2019**, *58*, 1880−1891.

(10) Scheiner, S. The Pnicogen Bond: Its Relation to Hydrogen, Halogen, and Other Noncovalent Bonds. *Acc. Chem. Res.* **2013**, *46*, 280−288.

(11) Wang, C.; Aman, Y.; Ji, X.; Mo, Y. Tetrel bonding interaction: an analysis with the block-localized wavefunction (BLW) approach. *Phys. Chem. Chem. Phys.* **2019**, *21*, 11776−11784.

(12) Dong, W.; Li, Q.; Scheiner, S. Comparative Strengths of Tetrel, Pnicogen, Chalcogen and Halogen Bonds and Contributing Factors. *Molecules* **2018**, *23*, 1681.

(13) Del Bene, J. E.; Alkorta, I.; Elguero, J. Do Traditional, Chlorine shared, and Ion-pair Halogen Bonds Exist? An ab Initio Investigation of FCl:CNX Complexes. *J. Phys. Chem. A* **2010**, *114*, 12958−12962.

(14) Del Bene, J. E.; Alkorta, I.; Elguero, J. An ab initio Study of Cooperative Effects In Ternary Complexes X:CNH:Z with X, Z=CNH, FH, ClH, FCl, and HLi: structures, binding energies, and spin-spin coupling constants across intermolecular bonds. *Phys. Chem. Chem. Phys.* **2011**, *13*, 13951−13961.

(15) Jiao, Y.; Liu, Y.; Zhao, W.; Wang, Z.; Ding, X.; Liu, H.; Lu, T. Theoretical Study on the Interactions of halogen-bonds and pnicogen-bonds in phosphine derivatives with Br_2, BrCl and BrF. *Int. J. Quant. Chem.* **2017**, *117*, No. e25443.

(16) Xu, H.; Cheng, J.; Li, Q.; Li, W. Some measures for making a traditional halogen bond be chlorine shared or ion-pair one in $FCl{\cdot}NH_3$ complex. *Mol. Phys.* **2016**, *114*, 3643−3649.

(17) Alkorta, I.; Sanchez-Sanz, G.; Elguero, J.; Del Bene, J. E. FCl:PCX Complexes: Old and New Types of Halogen Bonds. *J. Phys. Chem. A* **2012**, *116*, 2300−2308.
(18) Del Bene, J. E.; Alkorta, I.; Elguero, J. Influence of Substituent Effects on the Formation of P···Cl Pnicogen Bonds or Halogen Bonds. *J. Phys. Chem. A* **2014**, *118*, 2360−2366.
(19) Alkorta, I.; Elguero, J.; Del Bene, J. E. Characterizing Traditional and Chlorine-Shared Halogen Bonds in Complexes of Phosphine Derivatives with ClF and Cl_2. *J. Phys. Chem. A* **2014**, *118*, 4222−4231.
(20) Alkorta, I.; Elguero, J.; Mó, O.; Yáñez, M.; Del Bene, J. E. Using beryllium bonds to change halogen bonds from traditional to chlorine-shared to ion-pair bonds. *Phys. Chem. Chem. Phys.* **2015**, *17*, 2259−2267.
(21) Li, Z.; An, X. Strengthening of halogen bond in XCl...FH...F^- through cooperativity with a strong hydrogen bond and proton transfer. *J. Mol. Graphs. Model.* **2020**, *100*, 107673.
(22) Li, Q.; Ma, S.; Liu, X.; Li, W.; Cheng. Cooperative and substitution effects in enhancing strength of halogen bonds in FCl...CNX complexes. *J. Chem. Phys.* **2012**, *137*, 084314.
(23) Sutradhar, D.; Chandra, A. K. Halogen bonding between substituted Chlorobenzene and trimethylamine: Decisive role of σ-hole and C-Cl bond breaking energy. *Int. J. Quant. Chem.* **2018**, *118*, No. e25511.
(24) Sutradhar, D.; Chandra, A. K.; Zeegers-Huyskens, T. Theoretical study of the interaction of fluorinated dimethyl ethers and ClF and HF molecules. Comparison between halogen and hydrogen bonds. *Int. J. Quant. Chem.* **2016**, *116*, 670−680.
(25) Wang, P.; Zhao, N.; Tang, Y. Halogen Bonding in the Complexes of CH_3I and CCl_4 with Oxygen-Containing Halogen-Bond Acceptors. *J. Phys. Chem. A* **2017**, *121*, 5045−5055.
(26) Hauchecorne, D.; Moiana, A.; van der Veken, B. J.; Herrebout, W. A. Halogen binding to a divalent sulfur atom: an experimental study of the interaction of CF_3X (X = Cl, Br, I) with dimethyl sulfide. *Phys. Chem. Chem. Phys.* **2011**, *13*, 10204−10213.
(27) Ford, M. C.; Saxton, M.; Ho, P. S. Sulfur as a Acceptor to Bromine in Biomolecular Halogen Bonds. *J. Phys. Chem. Lett.* **2017**, *8*, 4246−4252.
(28) Oliveira, V.; Kraka, E.; Cremer, D. The intrinsic strength of the halogen bond: electrostatic and covalent contributions described by coupled cluster theory. *Phys. Chem. Chem. Phys.* **2016**, *18*, 33031−33046.
(29) Xu, Y.; Huang, J.; Gabidullin, B.; Bryce, D. L. A rare example of a phosphine as a halogen bond acceptor. *Chem. Commun.* **2018**, *54*, 11041−11043.
(30) Núñez, R.; Farràs, P.; Teixidor, F.; Viñas, C.; Sillanpää, R.; Kivekäs, R. A Discrete P···I-I···P Assembly: The Large Influence of weak Interactions on the 31P NMR Spectra of Phosphine-Diiodine Complexes. *Angew. Chem., Int. Ed.* **2006**, *45*, 1270−1272.
(31) Moussa, M. E.; Peresypkina, E.; Virovets, A.; Venus, D.; Balázs, G.; Scheer, M. Tuning the dimensionality of organometallic−organic hybrid polymers assembled from $[Cp_2Mo_2(CO)_4(\eta^2\text{-}P_2)]$, bipyridyl linkers and Ag^I ions. *CrystEngComm* **2018**, *20*, 7417−7422.
(32) Junk, P. C.; Atwood, J. L. Hydrogen bonded tetramethylethylenediammonium and triphenyl phosphonium complexes derived from liquid clathrate media. *J. Coord. Chem.* **1999**, *46*, 505−518.
(33) Fleischmann, M.; Heindl, C.; Seidl, M.; Balázs, G.; Virovets, A. V.; Peresypkina, E. V.; Tsunoda, M.; Gabbaï, F. P.; Scheer, M. Discrete and Extended Super sandwich Structures Based on Weak Interactions between Phosphorus and Mercury. *Angew. Chem., Int. Ed.* **2012**, *51*, 9918−9921.
(34) Holthausen, M. H.; Feldmann, K.-O.; Schulz, S.; Hepp, A.; Weigand, J. J. Formation of Cationic $[RP_5\text{-}Cl]^+$- Cages via Insertion of $[RPCl]^+$- Cations into a P-P bond of the P_4 Tetrahedron. *Inorg. Chem.* **2012**, *51*, 3374−3387.
(35) Pan, B.; Xu, Z.; Bezpalko, M. W.; Foxman, B. M.; Thomas, C. M. N-Heterocyclic Phosphenium Ligands as Sterically and electronically-Tunable Isolobal Analogues of Nitrosyls. *Inorg. Chem.* **2012**, *51*, 4170−4179.
(36) Reiling, S.; Besnard, M.; Bopp, P. A. Theoretical Studies on the Pyridine-I_2 Charge- Transfer Complex. 1. Ab-Initio Calculations on I_2 and Pyridine-I_2. *J. Phys. Chem. A* **1997**, *101*, 4409−4415.
(37) Wang, Z.; Zheng, B.; Yu, X.; Li, X.; Yi, P. Structure, properties, and nature of the pyridine-XY (X, Y= F, Cl, Br) complexes. *J. Chem. Phys.* **2010**, *132*, 164104.
(38) Anderson, L. N.; Aquino, F. W.; Raeber, A. E.; Chen, X.; Wong, B. M. Halogen Bonding Interactions: Revised Benchmarks and a New Assessment of Exchange vs Dispersion. *J. Chem. Theory Comput.* **2018**, *14*, 180−190.
(39) Poleshchuk, O. Kh.; Fateev, A. V.; Yarkova, A. G.; Ermakhanov, M. N.; Saidakhmetov, P. A. Study of Chemical bonding in the interhalogen complexes based on density functional theory. *Hyperfine Interact.* **2016**, *234*, 144.
(40) Hawthrone, B.; Fan-Hagenstein, H.; Wood, E.; Smith, J.; Hanks, T. Study of the Halogen Bonding between Pyridine and Perfluoroalkyl Iodide in Solution Phase using the Combination of FTIR and ^{19}F NMR. *Int. J. Spectrosc.* **2013**, 216518.
(41) Lias, S. G.; Bartmess, J. E.; Liebman, J. F.; Holmes, J. L.; Levine, Rh. D. Gas-phase ion and neutral thermochemistry. *J. Phys. Chem.* **1988**, *17*, 1−861.
(42) Batich, C.; Heilbronner, E.; Hornung, V.; Ashe, A. J.; Clark, D. T.; Cobley, U. T.; Kilcast, D.; Scanlan, I. Applications of photoelectron spectroscopy. 41. Photoelectron spectra of phospha-benzene, arsabenzene, andstibabenzene. *J. Am. Chem. Soc.* **1973**, *95*, 928−930.
(43) Cremer, D.; Kraka, E. Chemical Bonds without Bonding Electron Density — Does the Difference Electron-Density Analysis Suffice for a Description of the Chemical Bond? *Angew. Chem., Int. Ed.* **1984**, *23*, 627−628.
(44) (a) Macchi, P.; Proserpio, D. M.; Sironi, A. Experimental electron Density in a Transition Metal Dimer: Metal-Metal and Metal-Ligand Bonds. *J. Am. Chem. Soc.* **1998**, *120*, 13429−13435. (b) Macchi, P.; Garlaschelli, L.; Martinengo, S.; Sironi, A. Charge Density in Transition Metal Cluster: Supported vs Unsupported Metal-Metal Interactions. *J. Am. Chem. Soc.* **1999**, *121*, 10428−10429. (c) Novozhilova, I. V.; Volkov, A. V.; Coppens, P. Theoretical Analysis of the Triplet Excited State of the $[Pt_2(H_2P_2O_5)_4]^{4-}$ Ion and Comparison with Time-Resolved X-ray and Spectroscopic Results. *J. Am. Chem. Soc.* **2003**, *125*, 1079−1087. (d) Farrugia, L. J.; Senn, H. M. Metal−Metal and Metal−Ligand Bonding at a QTAIM Catastrophe: A Combined Experimental and Theoretical Charge Density Study on the Alkylidyne Cluster Fe3(μ-H)(μ-COMe)(CO)-10. *J. Phys. Chem. A* **2010**, *114*, 13418−13433.
(45) Sutradhar, D.; Bhattarai, S.; Zeegers-Huyskens, T.; Chandra, A. K. Unusual Fluorine Substitution Effect on S···Cl bonding between Sulphides and atomic Chlorine. *J. Phys. Chem. A* **2018**, *122*, 7142−7150.
(46) (a) Koch, U.; Popelier, P. L. A. Characterization of C-H-O bonds on the basis of the charge density. *J. Chem. Phys.* **1995**, *99*, 9747−9754. (b) Popelier, P. L. A. Characterization of a dihydrogen bond on the basis of the charge density. *J. Phys. Chem. A* **1998**, *102*, 1873−1878.
(47) Bent, H. A. An Appraisal of Valence-bond Structures and Hybridization in Compounds of the First-row elements. *Chem. Rev.* **1961**, *61*, 275−311.
(48) Sutradhar, D.; Chandra, A. K.; Zeegers-Huyskens, T. Theoretical Study of the Interaction of Fluorinated Dimethyl Ethers and the ClF and HF Molecules. Comparison between Halogen and Hydrogen Bonds. *Int. J. Quant. Chem.* **2016**, *116*, 670−680.
(49) Badger, R. M.; Bauer, S. H. Spectroscopic Studies of the Hydrogen Bond. II. The Shift of the O-H Vibrational Frequency in the Formation of the Hydrogen Bond. *Chem. Phys.* **1937**, *5*, 839−851.
(50) Sutradhar, D.; Zeegers-Huyskens, T.; Chandra, A. K. Theoretical study of the interaction between pyridine derivatives and atomic chlorine. Substituent effect and nature of the bonding. *Mol. Phys.* **2015**, *113*, 3232−3240.

https://dx.doi.org/10.1021/acsomega.0c03567
ACS Omega 2020, 5, 24095−24105

(51) Boys, S. F.; Bernardi, F. The Calculation of small molecular interactions by the differences of separate total energies. Some procedures with reduced errors. *Mol. Phys.* **1970**, *19*, 553−566.
(52) Reed, A. E.; Curtiss, L. A.; Weinhold, F. Intermolecular Interactions from a Natural Bond Orbital, Donor-Acceptor Viewpoint. *Chem. Rev.* **1988**, *88*, 899−926.
(53) Bader, R. F. W. *Atoms in Molecules: A Quantum Theory*, 1st ed.; The International Series of Monographs on Chemistry; Oxford University Press: Oxford, 1994; Vol. *22*.
(54) Bulat, F. A.; Toro-Labbé, A.; Brinck, T.; Murray, J. S.; Politzer, P. Quantitative analysis of molecular surfaces: areas, volumes, electrostatic potentials and average local ionization energies. *J. Mol. Model.* **2010**, *16*, 1679−1691.
(55) Turney, J. M.; Simmonett, A. C.; Parrish, R. M.; Hohenstein, E. G.; Evangelista, F. A.; Fermann, J. T.; Mintz, B. J.; Burns, L. A.; Wilke, J. J.; Abrams, M. L.; et al. Psi4: An open-source ab initio electronic structure Program. *Wiley Interdiscip. Rev.: Comput. Mol. Sci.* **2012**, *2*, 556−565.
(56) Frisch, M. J.; Trucks, G. W.; Schlegel, H. B.; Scuseria, G. E.; Robb, M. A.; Cheeseman, J. R.; Scalmani, G.; Barone, V.; Mennucci, B.; Petersson, G. A.; Nakatsuji, H.; Caricato, M.; Li, X.; Hratchian, H. P.; Izmaylov, A. F.; Bloino, J.; Zheng, G.; Sonnenberg, J. L.; Hada, M.; Ehara, M.; Toyota, K.; Fukuda, R.; Hasegawa, J.; Ishida, M.; Nakajima, T.; Honda, Y.; Kitao, O.; Nakai, H.; Vreven, T.; Montgomery, J. A., Jr.; Peralta, J. E.; Ogliaro, F.; Bearpark, M.; Heyd, J. J.; Brothers, E.; Kudin, K. N.; Staroverov, V. N.; Kobayashi, R.; Normand, J.; Raghavachari, K.; Rendell, A.; Burant, J. C.; Iyengar, S. S.; Tomasi, J.; Cossi, M.; Rega, N.; Millam, N. J.; Klene, M.; Knox, J. E.; Cross, J. B.; Bakken, V.; Adamo, C.; Jaramillo, J.; Gomperts, R.; Stratmann, R. E.; Yazyev, O.; Austin, A. J.; Cammi, R.; Pomelli, C.; Ochterski, J. W.; Martin, R. L.; Morokuma, K.; Zakrzewski, V. G.; Voth, G. A.; Salvador, P.; Dannenberg, J. J.; Dapprich, S.; Daniels, A. D.; Farkas, Ö.; Foresman, J. B.; Ortiz, J. V.; Cioslowski, J.; Fox, D. J. *Gaussian 09*, Revision C.01; Gaussian, Inc.: Wallingford, CT, 2009.

https://dx.doi.org/10.1021/acsomega.0c03567
ACS Omega 2020, 5, 24095−24105